

Editors

Thomas M. Moses | Shane F. McClure

DIAMOND

Natural Colorless Type IaB
Diamond with Silicon-Vacancy
Defect Center

The silicon-vacancy defect, or $[\text{Si-V}]^-$, is one of the most important features in identifying CVD synthetic diamonds. It can be effectively detected using laser photoluminescence technology to reveal sharp doublet emissions at 736.6 and 736.9 nm. This defect is extremely rare in natural diamonds (C.M. Breeding and W. Wang, "Occurrence of the Si-V defect center in natural colorless gem diamonds," *Diamond and Related Materials*, Vol. 17, No. 7–10, pp. 1335–1344) and has been detected in very few natural type IIa and IaAB diamonds over the past several years.

Recently, a 0.40 ct round brilliant diamond with D color and VS_2 clarity (figure 1) was submitted to the Hong Kong laboratory for grading service. It was identified as a pure type IaB natural diamond. Infrared absorption spectroscopy showed low concentrations of the hydrogen peak (3107 cm^{-1}) and N impurities in the B aggregates. Photoluminescence spectra at liquid-nitrogen temperature with 514 nm laser excitation revealed $[\text{Si-V}]^-$ doublet emissions at 736.6 and 736.9 nm (figure 2), while 457 nm laser excitation revealed the H3 (503.2 nm) emission. DiamondView fluorescence images



Figure 1. Emissions from the silicon-vacancy defect at 736.6 and 736.9 nm were detected in this 0.40 ct type IaB natural diamond.

showed blue fluorescence with natural diamond growth patterns. These gemo-

logical and spectroscopic features confirmed the diamond's natural origin, despite the occurrence of $[\text{Si-V}]^-$ emissions. No treatment was detected.

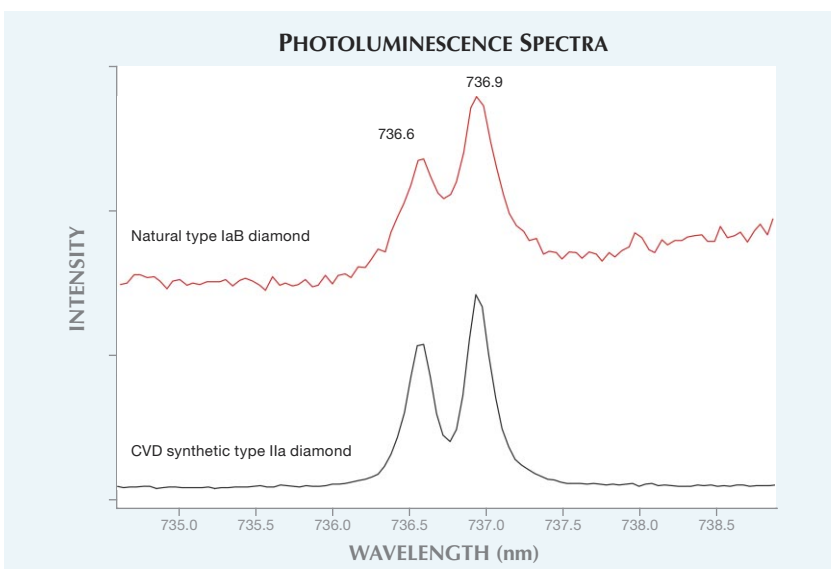
Examination of this stone indicated that the $[\text{Si-V}]^-$ defect can occur, albeit rarely, in multiple types of natural diamonds. Therefore, all properties should be carefully examined in reaching a conclusion when $[\text{Si-V}]^-$ is present.

Carmen "Wai Kar" Lo

Screening of Small Yellow Melee for
Treatment and Synthetics

Diamond treatment and synthesis have undergone significant developments in the last decade. During this time, the trade has grown increasingly concerned about the mixing of treated

Figure 2. The emission peaks at 736.6 and 736.9 nm from the $[\text{Si-V}]^-$ defect are shown in the type IaB diamond's photoluminescence spectrum. Identical peak positions are detected in CVD synthetic diamonds.



Editors' note: All items were written by staff members of GIA laboratories.

GEMS & GEMOLOGY, Vol. 50, No. 4, pp. 293–301.

© 2014 Gemological Institute of America

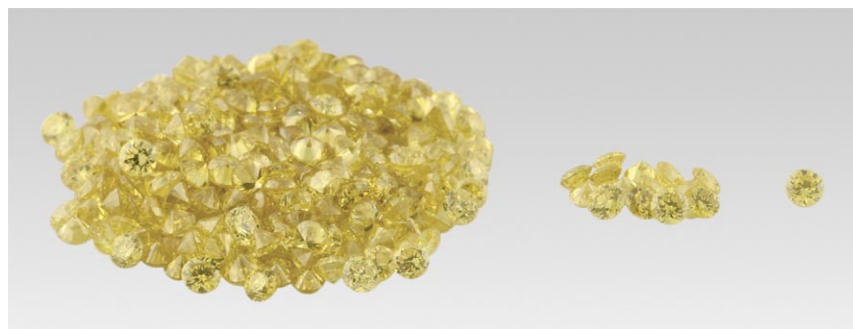


Figure 3. This group of 359 intensely colored round yellow diamonds (0.02–0.03 ct) was screened by GIA’s New York laboratory. Among these, the majority were natural (left), 14 were HPHT synthetics (middle), and one was HPHT-treated natural diamond (right). They all displayed uniform appearance and could not be distinguished visually.

and/or synthetic diamonds with natural melee-sized goods. Because it is often not feasible to test every small diamond in a parcel, many of these products could be traded without being tested individually by a gem lab. GIA’s New York laboratory recently tested two large groups of melee yellow diamonds submitted for screening of treatments and synthetics. The results will likely have profound implications for how melee diamonds are handled in the trade.

A parcel of 359 round diamonds between 0.02 and 0.03 ct was submitted for identification. They showed uniform appearance, intense yellow color, and good clarity. Based on spectroscopic analysis, each sample’s color was attributed to trace concentrations of isolated nitrogen. Gemological observations, infrared absorption spectroscopy, and DiamondView analysis confirmed that 344 of them were natural diamonds, 14 were grown by HPHT (high-pressure, high-temperature) synthesis, and one was an HPHT-treated natural diamond (figure 3).

Of the 14 synthetic diamonds, eight were dominated by A-aggregate form nitrogen with trace isolated nitrogen, while the other six showed negligible amounts. All had widespread pinpoint inclusions, a feature typical of HPHT synthetic diamonds. Characteristic growth features of HPHT synthesis were confirmed using a DiamondView fluorescence instrument on six of them. The synthetic diamonds with a high concentration of A-aggregate form nitrogen were produced at much higher temperatures, indicating more than one producer.

To gain perspective on the surprisingly high prevalence of synthetic

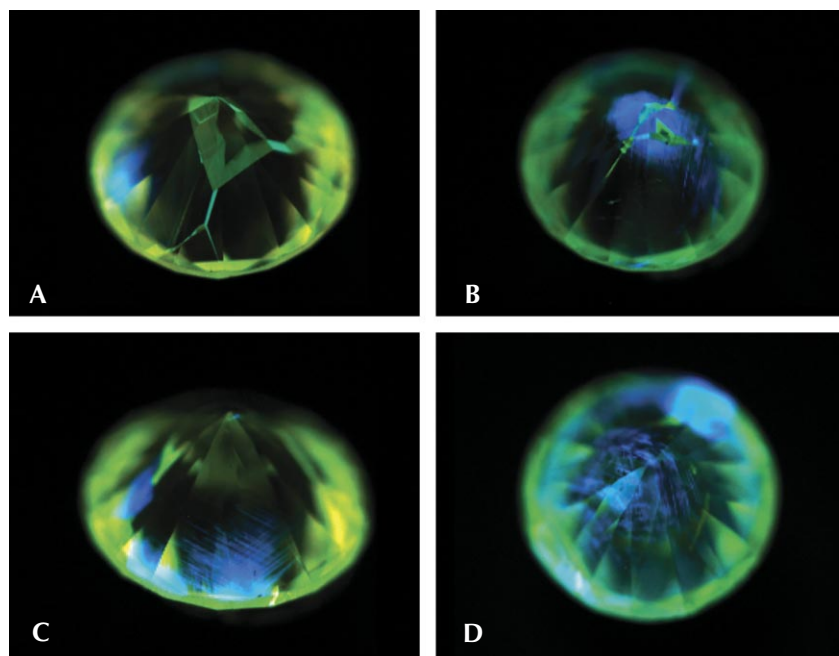
and treated diamonds found in this parcel, we analyzed an additional parcel containing 525 samples, with similar results. One of these was HPHT-processed, while 10 displayed the spectral, microscopic, and fluorescence characteristics typical of HPHT synthetics; we concluded that the remaining 514 were natural and untreated. Typical DiamondView characteristics of HPHT synthetics were observed, but most of the HPHT synthetics showed fluorescence patterns similar to those of natural diamonds (figure 4). This observation emphasizes the importance of infrared absorption spectroscopy, in addition to DiamondView imaging,

when determining diamond origin.

This study indicates that melee diamonds in the marketplace are being contaminated by synthetic and treated diamonds. Screening analysis by gem labs is essential to ensuring the correct identification. An efficient and reliable screening can be performed using infrared absorption spectroscopy, DiamondView fluorescence imagery, and optical microscopy. From our analysis of 883 melee samples in all, we concluded that 857 were natural diamond (97.1%), 24 were HPHT synthetic diamond (2.7%), and two were HPHT-processed natural diamonds (0.2%).

Wuyi Wang, Martha Altobelli, Caitlin Dieck, and Rachel Sheppard

Figure 4. These DiamondView fluorescence images show (A) growth sector patterns typical of HPHT synthetic diamonds, (B) HPHT treatment, and (C and D) uncharacteristic HPHT synthetic patterns.



Very Large Irradiated Yellow

Artificial irradiation, with or without annealing, has been used to improve the color of natural diamonds for several decades. This technique is usually applied to brownish or light yellow diamonds of relatively small size. The New York lab recently tested a very large yellow diamond that had been artificially irradiated.

This emerald-cut stone weighed 22.27 ct and was color graded as Fancy Vivid yellow (figure 5). Faint color concentration was observed along the culet. The diamond showed medium yellow-green, slightly chalky fluorescence to long-wave UV and weak orange fluorescence to short-wave UV. No obvious internal features were observed. Its infrared absorption spectrum showed high concentrations of nitrogen and weak absorptions from defects H1b (4935 cm^{-1}) and H1c (5165 cm^{-1}). A weak hydrogen-related absorption at 3107 cm^{-1} was also detected. In the Vis-NIR region, the absorption spectrum collected at liquid-nitrogen temperature showed strong absorptions from the N3, H4, H3, and 595 nm optical centers (figure 6). These spectroscopic and gemological features demonstrated that the diamond had been artificially irradiated and annealed to introduce additional absorptions from the H3/H4 defects,

Figure 5. This 22.27 ct Fancy Vivid yellow diamond was identified as artificially irradiated and annealed. Treated diamonds of this size and attractively saturated color are rare.

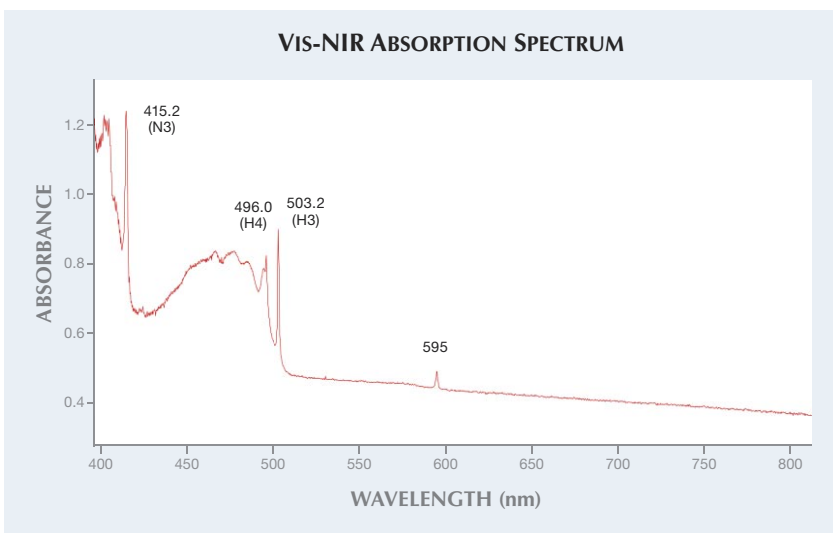
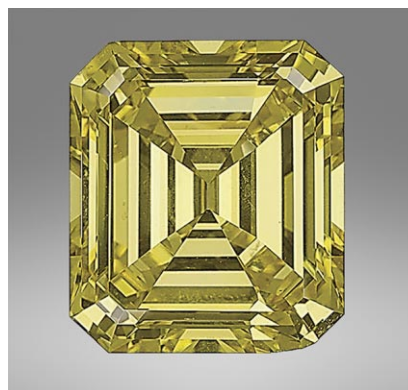


Figure 6. The irradiated yellow diamond's Vis-NIR absorption spectrum, collected at liquid-nitrogen temperature, showed strong absorption from the H3 and H4 defects, which were artificially introduced to enhance the yellow color.

enhancing its yellow color. This Fancy Vivid yellow color would have been much lighter and less saturated before the treatment.

Artificially irradiated diamonds of this size and attractive color are rarely examined in gem laboratories.

Wuyi Wang

Natural PEARL Aggregates from *Pteria* Mollusks

Both natural and cultured pearls of *Pteria*-species mollusks from the Gulf of California, Mexico (M. Cariño and M. Monteforte, "History of pearling in La Paz Bay, South Baja California," Summer 1995 *G&G*, pp. 88–104; L.

Kiefert et al., "Cultured pearls from the Gulf of California, Mexico," Spring 2004 *G&G*, pp. 26–38) are examined in GIA laboratories from time to time. But a recent submission to the New York lab of 10 loose pearls, ranging from 8.17 × 7.65 × 3.89 mm to 17.85 × 11.16 × 6.80 mm (figure 7), proved interesting owing to their shapes and internal growth features. All the pearls had a "grapelike" cluster appearance, as if multiple smaller pearls had combined into aggregates. Their colors ranged from dark brown and purple to gray, with strong orient consisting of mainly bluish and pinkish overtones.

Microscopic examination revealed that the pearls formed with continu-

Figure 7. These 10 loose natural pearl aggregates from the *Pteria* species ranged from dark brown and purple to gray.



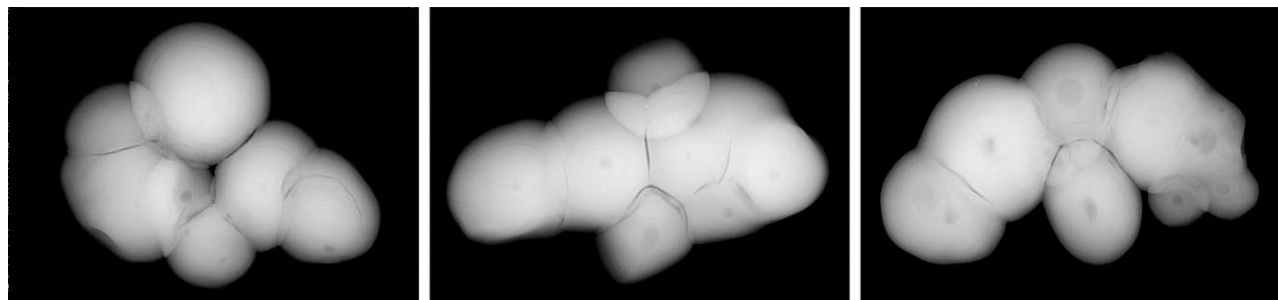


Figure 8. Microradiograph images of the pearls revealed multiple growth units with central conchiolin-rich cores in each unit.

ous nacre layers. Microradiography further demonstrated that their internal structures were composed of multiple small pearls related to their growth (figure 8). Conchiolin-rich centers were observed in all of the sub-units, indicating natural formation. Additional advanced testing (UV-Vis reflectance spectrophotometry, photoluminescence spectroscopy, and EDXRF spectrometry) showed that all 10 of the pearls had a natural color. More importantly, all 10 exhibited medium to strong orangy red to red fluorescence under long-wave UV, which is characteristic of pearls that form in *Pteria* mollusks (figure 9).

Pearls grown from the aggregation of smaller pearls are sometimes associated with freshwater culturing practices (Summer 2012 Lab Notes, pp. 138–139). Yet these samples clearly did not appear to be cultured. Our client later informed us that the pearls were obtained more than 40 years ago, reportedly off the Mexican

Figure 9. The pearls produced this striking characteristic red fluorescence under long-wave UV.



coast, which further supports the identity of these unique pieces.

Sally Chan and Yixin (Jessie) Zhou

Lead-Glass-Filled Burmese RUBIES

Rubies filled with a high-lead-content glass as a clarity enhancement were first reported by the Gemmological Association of All Japan (GAAJ) laboratory in 2004. Since then, many of these stones have been examined by gemological laboratories around the world. They are identified by their numerous large, low-relief fractures and their blue or orange flashes easily seen at different angles, as well as their

flattened gas bubbles and voids that are obvious under magnification (S.F. McClure et al., "Identification and durability of lead glass-filled rubies, Spring 2006 *G&G*, pp. 22–34).

The Carlsbad laboratory recently had the opportunity to examine a multi-strand necklace of graduated round ruby beads (figure 10), measuring 2.72 to 6.13 mm in diameter. Standard gemological testing showed properties consistent with natural ruby. Microscopic observations revealed typical inclusions for ruby: rutile silk, banded particulate clouds, twinning planes, red parallel planar zoning, and roiled graining. The ap-

Figure 10. The Burmese ruby beads in this multi-strand necklace were filled with lead glass.





Figure 11. These wide fractures, filled with glass of relatively low lead content, showed a slightly lower luster than the host ruby. Field of view 2.96 mm.

pearance and chemical composition of the beads suggested that their geographic origin was Mogok, Myanmar. Their wide, low-relief fractures (figure 11) and cavities were filled with a foreign substance whose luster was slightly lower than that of the rubies. These observations suggested a lead-glass filler, although the lower luster was contrary to previous documentation and the filler did not display any flash effect. In some beads, the filler also showed a crazed appearance (figure 12) not typically observed in other rubies filled with high-lead glass.

This strange observation prompted us to carry out a chemical analysis of the glass filler. We tested two spots using laser ablation–inductively coupled plasma–mass spectrometry (LA-ICP-MS) on a relatively large glass-filled cavity. The results after normal-

Figure 12. In some beads, the filler also showed a crazed appearance not typically observed in other rubies filled with lead glass. Field of view 2.96 mm.

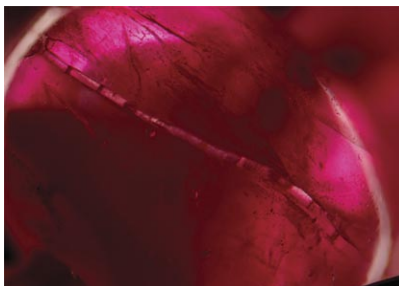


Figure 13. Some beads were so highly fractured and filled that they would be called “manufactured products consisting of lead glass and ruby.” This material would easily disintegrate if the lead glass were removed. Field of view 2.96 mm.

ization showed that the filler contained approximately 43 wt.% PbO, which was much lower than the lead content reported by McClure et al. in 2006 (71–76 wt.%). The diminished lead content would lower the refractive index of the glass and explain the lack of flash effect and the lower luster observed in this filler.

These beads were the first examples of this lower-lead-content glass filling in Burmese rubies examined at the Carlsbad laboratory. On a GIA report, most of these beads would be identified as “rubies with significant clarity enhancement with lead glass filler.” Yet some of the beads were so highly fractured and filled that they would be considered “manufactured products consisting of lead glass and ruby” (figure 13).

Najmeh Anjomani and
Rebecca Tsang

Spinel Inclusion in SPINEL

A 26.73 ct transparent dark pink-purple oval mixed cut (figure 14) was submitted to the Carlsbad laboratory for identification services. Standard gemological testing showed a refractive index of 1.719 and a hydrostatic specific gravity of 3.59. The stone fluoresced very weak red to long-wave UV light and was inert to short-wave



Figure 14. This 26.73 ct dark pink-purple spinel contained a spinel crystal inclusion.

UV. Observed using a handheld spectroscope, the stone showed thin absorption bands near 680 nm, with fine absorption lines near 670 nm. These gemological properties were consistent with spinel.

Interestingly, microscopic examination showed that the spinel was relatively free of inclusions except for a very low-relief solid inclusion that was only partially visible (figure 15). Examination with polarized light (figure 16) revealed the entire outline of the low-relief crystal. Unaltered crystals generally provide strong evidence that a stone has not been heated, and this inclusion showed no alteration. But it is also important to consider the identity of certain inclusions when using them as an indication for thermal treatment. Due to the low re-

Figure 15. Under diffused lighting, the outline of the spinel crystal was only partially visible. Image width 3.70 mm.





Figure 16. Under polarized lighting, the outline of the spinel crystal was clearly visible. Image width 3.70 mm.

lie of this inclusion, it is very likely a spinel inside of spinel. Their matching refractive index explains why the inclusion is nearly invisible. Since the host and inclusion are the same material, we would not expect to see any alteration due to heat treatment. Therefore, the unaltered appearance of this inclusion cannot be used to determine that this spinel has not been heat treated.

The spinel's visible absorption spectrum revealed that its purple color results from the combination of Fe and Cr (figure 17). Absorption bands with a maximum at 400 and 550 nm are caused by Cr^{3+} (D.L. Wood

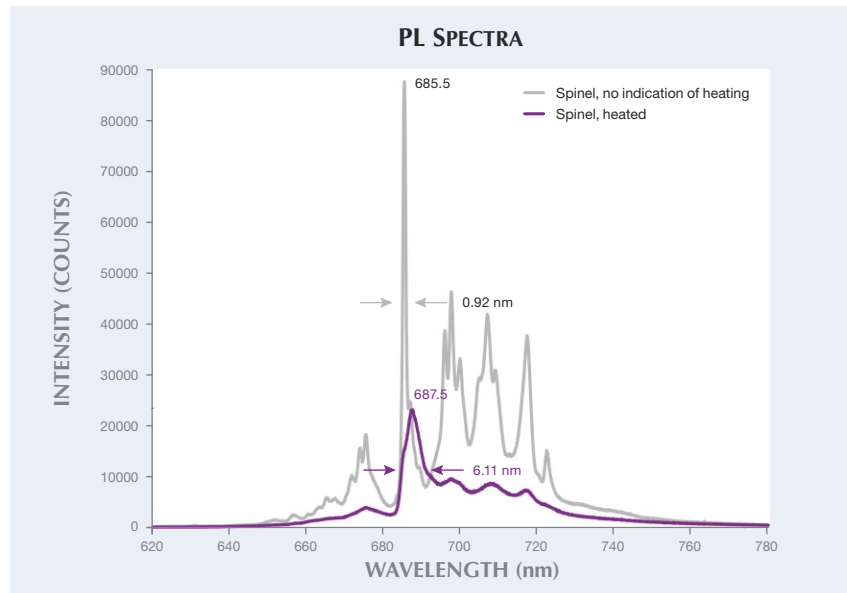
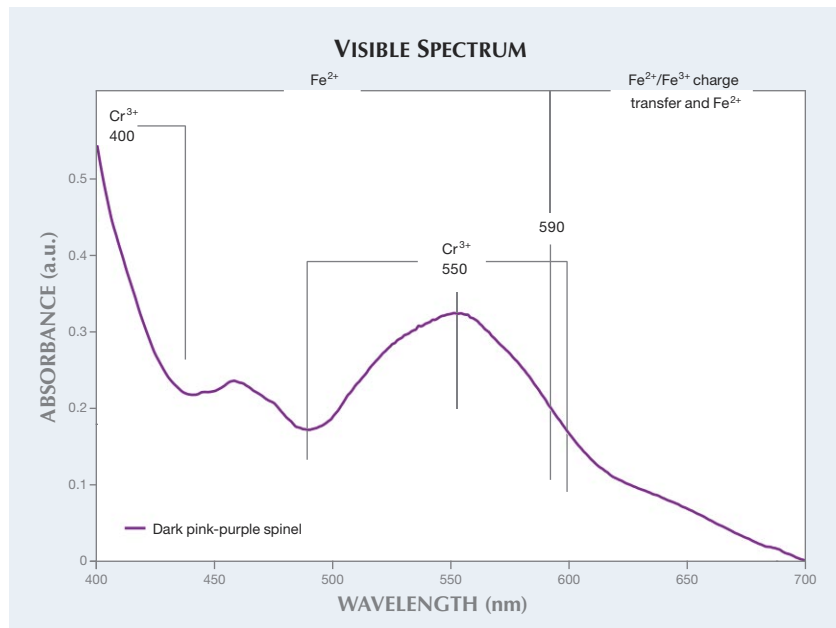


Figure 18. The gray spectrum of unheated spinel shows that the FWHM (full width at half maximum) of the peak with highest counts is 0.92 nm and the position of the peak is at 685.5 nm. The purple spectrum, representing the dark pink-purple spinel, shows that the FWHM of the peak with highest counts is 6.11 nm and the peak is shifted from 685.5 to 687.5 nm.

et al., "Optical spectrum of Cr^{3+} ions in spinels," *The Journal of Chemical Physics*, Vol. 48, No. 11, 1968, pp. 5255–5262). Fe^{2+} causes the absorption band from 400 to 590 nm, while

the $\text{Fe}^{2+}/\text{Fe}^{3+}$ charge transfer and Fe^{2+} cause the absorption bands from 590 to 700 nm (S. Muhlmeister et al., "Flux-grown synthetic red and blue spinels from Russia," Summer 1993 *GeJG*, pp. 81–98).

Figure 17. The spinel's visible spectrum revealed that its dark pink-purple color was caused by Cr and Fe.



Spinel submitted to GIA's laboratory are routinely checked using advanced analytical tools. Laser ablation-inductively coupled plasma-mass spectrometry (LA-ICP-MS) was used to confirm the natural trace elements. Higher concentrations of Li (27.7 ppmw), Be (87.4 ppmw), Zn (133 ppmw), and Ga (63 ppmw) indicate a natural origin, and the specimen's photoluminescence (PL) spectrum was consistent with a heated spinel due to the broad full width at half maximum (FWHM) observed at 687.5 nm (figure 18; see S. Saeseaw et al., "Distinguishing heated spinels from unheated natural spinels and from synthetic spinels," GIA Research News, April 2009, <http://www.gia.edu/gia-news-research-NR32209A>). It was unusual to see a spinel with this dark pink-purple color showing evidence of heat, as we typically see only red spinels that have been heated. From careful microscopic examination and

advanced gemological testing, we were able to conclude that this was a natural spinel showing indications of heating.

Amy Cooper and Ziyin Sun

CVD SYNTHETIC DIAMOND with Fancy Vivid Orange Color

With the rapid improvement of CVD synthetic diamond quality in recent years, various colorations can be introduced after growth. The New York laboratory recently tested a CVD synthetic with a very attractive orange color.

This round-cut specimen weighed 1.04 ct and was color graded as Fancy Vivid pinkish orange (figure 19), a very rare color among natural and treated diamonds. Except for a few dark pin-point inclusions, it showed no notable internal features. Under crossed polarizers, it displayed natural-looking “tatami” strain patterns. Absorption spectroscopy in the infrared region showed typical type IIa features, with no detectable defect-related absorption. At liquid-nitrogen temperature, a few absorption features were detected in the UV-Vis-NIR region (figure 20). The major ones include absorptions from N-V centers with ZPL at 575.0 and 636.9 nm, and their

Figure 19. This 1.04 ct round was identified as a CVD synthetic diamond. Its Fancy Vivid pinkish orange color was introduced through post-growth irradiation and annealing.

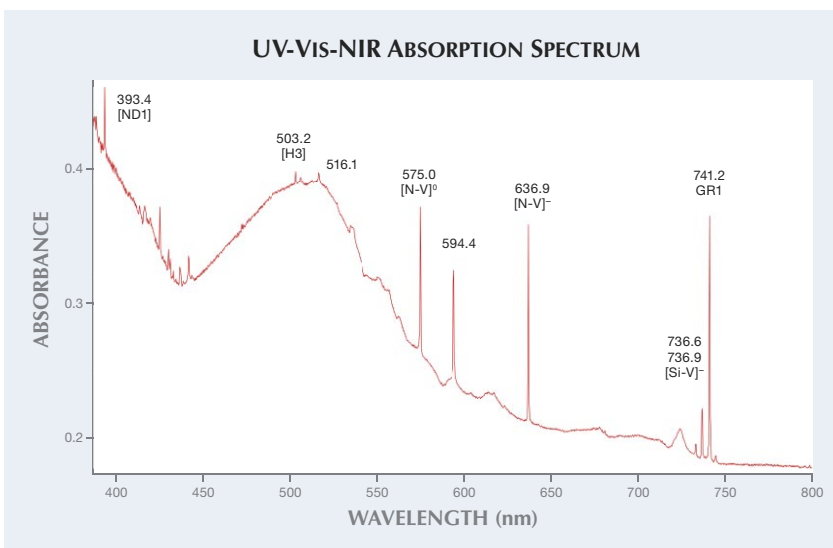


Figure 20. Several defects were detected in the CVD synthetic diamond's absorption spectrum in the UV-Vis-NIR region at liquid-nitrogen temperature. Strong absorptions from the N-V centers are the main cause of the observed pinkish orange color.

related side bands. We also recorded absorptions from some irradiation-related defects, including 594.4 nm, GR1 at 741.2 nm, ND1 at 393.4 nm, and the general radiation absorption features at 420–450 nm. Also observed were weak absorptions from the H3 defect at 503.2 nm, possible nickel-related defects at 516.1 nm, and [Si-V]⁻ at 736.6/736.9 nm. Under the strong short-wave UV radiation of the DiamondView, the sample showed very strong red fluorescence with sharp linear growth striations, a unique feature of CVD synthetic diamond. Weak red phosphorescence was also detected. These observations confirmed that this was a CVD synthetic diamond with post-growth treatments. Nitrogen concentration, based on absorptions in infrared absorption spectroscopy, was below 1 ppm. After initial growth, the sample was artificially irradiated and then annealed at moderate temperatures to introduce the N-V centers. Strong absorptions from N-V centers are the main causes of the observed pinkish orange bodycolor.

The very attractive orange color was achieved by introducing the proper concentrations of N-V centers while limiting the formation of other defects. It should be pointed out that

the relatively high concentration of [Si-V]⁻ could be attributed to the treatment by combining preexisting Si impurity with artificially introduced vacancies. With further developments in after-growth treatment, it is highly likely that more colors in CVD synthetic diamonds will be introduced.

Wuyi Wang and Kyaw Soe Moe

Mixed-Type HPHT SYNTHETIC DIAMOND with Unusual Growth Features

A 0.28 ct round brilliant was submitted as synthetic moissanite to the Carlsbad lab for an identification report. At first glance, synthetic moissanite seemed like a possibility. The stone had a green-yellow color and contained numerous growth tubes visible through the table (figure 21). Yet it did not show doubling in the microscope, which is a characteristic feature of synthetic moissanite. Its infrared spectrum was a match for diamond. The infrared spectrum also showed a very unusual combination of boron and nitrogen impurities at 2804 and 1130 cm⁻¹, respectively (figure 22). These two impurities are not known to occur together in natural diamonds in measurable quantities.



Figure 21. These growth tube features were visible through the table of the HPHT-grown synthetic diamond. Magnified approximately 90 \times .

This was a strong indicator of synthetic origin. A DiamondView image (figure 23) confirmed that it was synthetic, grown by the high-pressure, high-temperature (HPHT) method. It is noteworthy that after the sample was removed from the DiamondView, it showed very strong blue phosphorescence that was clearly visible in ambient room lighting and persisted for several minutes.

Unless special precautions are taken, diamond synthesis will incorporate nitrogen into the lattice, which leads to a yellow bodycolor. Certain chemicals can be added to prevent the incorporation of nitrogen, and this can lead to colorless diamonds. If boron is introduced to the growth of synthetic diamonds, it will become incorporated and produce a blue bodycolor. If both

Figure 23. This DiamondView image shows the characteristic growth pattern of an HPHT synthetic diamond.

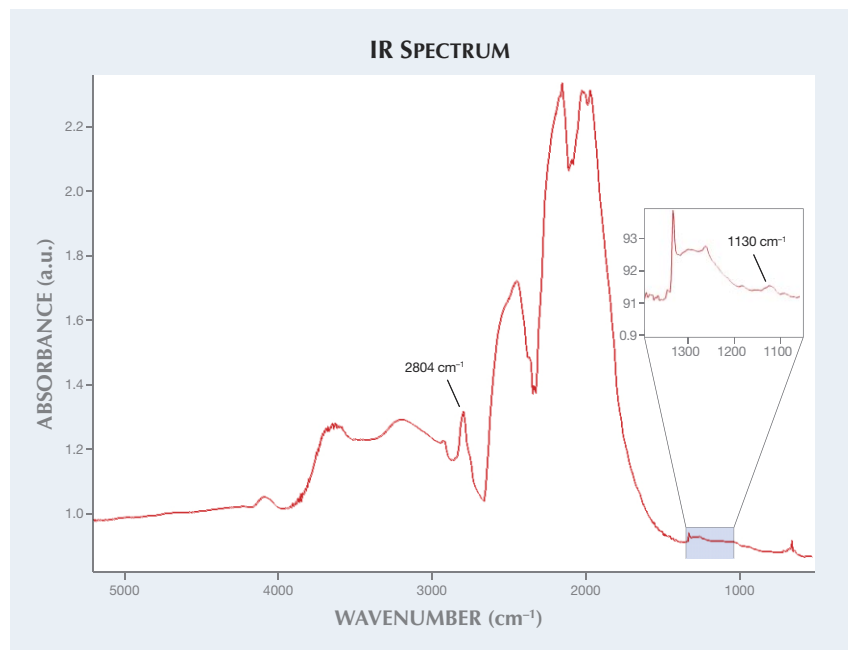


Figure 22. The HPHT-grown synthetic diamond's infrared spectrum shows peaks related to both boron and single nitrogen.

boron and nitrogen are allowed to incorporate into the lattice, the blue and yellow bodycolors will combine to produce a green color (J.E. Shigley et al., "Lab-grown colored diamonds from Chatham Created Gems," Summer 2004 *G&G*, pp. 128–145). Since boron is an electron acceptor and nitrogen is an electron donor, an excess of boron will compensate the nitrogen and the blue color will predominate. Because nitrogen and boron have slight preferences for different growth sectors, if the concentration of both nitrogen and boron is carefully controlled, nitrogen and boron will dominate different growth sectors. The colors will blend to create a face-up greenish color (R.C. Burns et al., "Growth-sector dependence of optical features in large synthetic diamonds," *Journal of Crystal Growth*, Vol. 104, No. 2, 1990, pp. 257–279).

The growth tubes in this sample were an unusual feature, last seen in a selection of HPHT-grown synthetics several years ago at GIA's West Coast laboratory. They appear similar to synthetic moissanite growth tubes, though there are a few key differences. Whereas the growth tubes occur in only one direction in syn-

thetic moissanite, they could be seen growing in different directions in this synthetic diamond. The tubes in synthetic moissanite also tend to be very straight, while the ones in this sample curved and changed direction. Although this stone bore some superficial resemblance to moissanite, its gemological properties were quite different, another reminder to avoid quick sight identifications.

Troy Ardon

A Larger, Higher-Quality NPD SYNTHETIC DIAMOND

In February 2014, these authors reported the first example of a synthetic nano-polycrystalline diamond (NPD) detected by a gemological laboratory (see www.gia.edu/gia-news-research-fancy-black-NPD-synthetic). The 0.9 ct marquise was small and so heavily included with graphite crystals as to receive a Fancy Black color grade. The East Coast laboratory recently detected another undisclosed NPD synthetic diamond, a 1.51 ct Fancy Black round.

This NPD specimen was larger and had a much better transparency than the previous NPD, though it still



Figure 24. This 1.51 ct Fancy Black nano-polycrystalline diamond (NPD) synthetic, submitted undisclosed, was larger and showed much better transparency than a previously detected NPD synthetic.

graded as Fancy Black (figure 24). Infrared spectroscopy showed a diagnostic absorption pattern for diamond, with strong absorption in the one-phonon region (approximately 400–1332 cm^{-1}). Absorption in this region is usually attributed to nitrogen impurity in different aggregation states, but careful observation showed otherwise.

The specimen's infrared absorption pattern matched that of known NPD samples (figure 25). Further testing, including Raman spectroscopy and DiamondView imaging, confirmed the

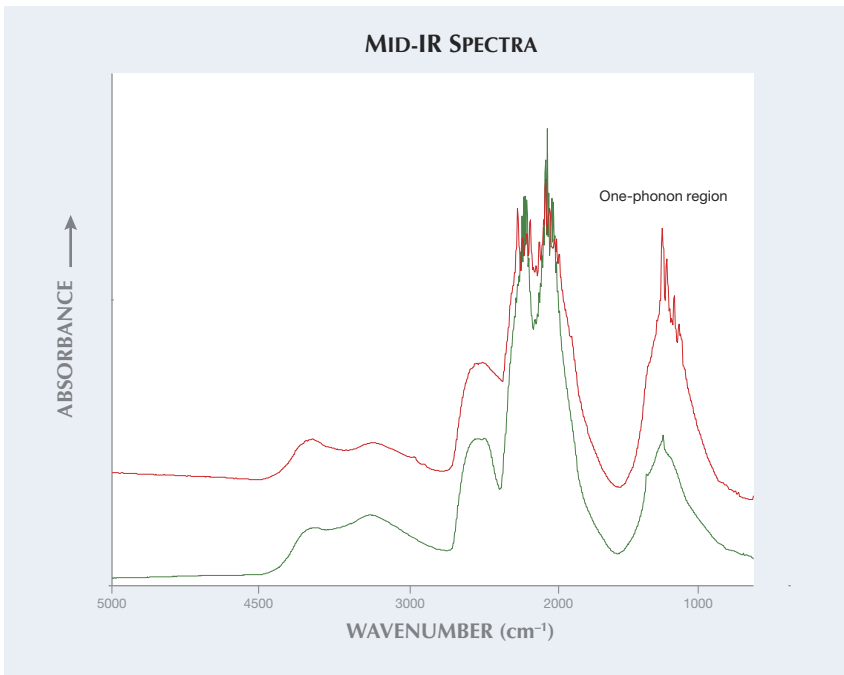


Figure 25. The mid-FTIR spectrum of the 1.51 ct black NPD synthetic diamond (red) displayed absorption in the one-phonon region similar to that of known NPD samples (green).

sample to be a NPD synthetic diamond. Microscopic observation revealed that the host material had the yellow color typical of previously reported NPD samples (see E.A. Skalwold, "Nano-polycrystalline diamond sphere: A gemologist's perspective," Summer 2012 *G&G*, pp. 128–131). The sample was heavily in-

cluded with graphite, but less so than the previously reported 0.9 ct marquise, and therefore it had a better transparency (figure 26).

The origin of this synthetic diamond is not known, but it showed obvious improvements in size and quality compared to the marquise reported in February 2014. In the future, NPD synthetics could pose an identification challenge to the gem and jewelry industry. Careful gemological observations and advanced testing techniques were required to identify this undisclosed synthetic diamond.

Paul Johnson and Kyaw Soe Moe

Figure 26. These photomicrographs, magnified 35 \times (left) and 40 \times (right), show abundant inclusions of graphite inclusions. Note the yellow color of the host material.

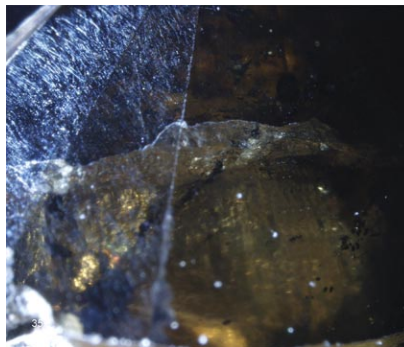


PHOTO CREDITS:

Johnny Leung—1; Sood Oil (Judy) Chia—3, 5, 7, 19; Martha Altobelli and Caitlin Dieck—4; Yixin (Jessie) Zhou—8; Jian Xin (Jae) Liao—9, 24; C.D. Mengason—10; Nathan Renfro—11–13; Robison McMurtry—14; Ziyin Sun—15, 16; Troy Ardon—21, 23; Paul Johnson—26.